

Modelling and Simulation of 6 Pulse GTO Thyristor Converter

Muhamad Zahim Sujod
*University Malaysia Pahang
Malaysia*

1. Introduction

Conventional thyristor (known as SCR) has been used in various applications such as in power converter of high voltage direct current (hvdc) transmission system and as a dc speed controller for dc motor application (F. Schettler et al., 2000). Conventional thyristor can only be turned on with two conditions, that is when the device is in forward blocking state or when positive gate current is applied at the gate. This thyristor cannot be turned off by applying negative gate current. It can only be turned off if anode current goes negative (reverse). This happens when negative portion of the sine wave occurs (natural commutation). Another method of turning off is known as "forced commutation" where anode current is "diverted" to another circuitry. Alternatively, we have Gate Turn-Off (GTO) thyristor to overcome the disadvantage of conventional thyristor. GTO thyristor behave like conventional thyristor, but can be turned off using gate signal. It needs very large reverse gate current (normally 1/5 of anode current) to turn-off. Since a GTO thyristor converter is self-commutated, it can be used to supply power to a weak ac system, and even to a "load-only" system. At the same time, it is able to control reactive power from lead to lag to keep an ac bus voltage constant.

In this paper, we create a model of GTO thyristor with its operation circuit and gate circuit using OrCAD PSPICE simulator and make an analysis of their switching characteristics at different anode currents. Then, this GTO thyristor model is used and implemented in the 6 pulse converter circuit. Finally, we compare the simulation results of dc output voltage with mathematical calculation results.

2. GTO thyristor model

In the library of OrCAD PSPICE simulator, GTO thyristor model is not included. So, we use two transistor models to create GTO thyristor model for the simulation. The monolithic npnp structure of GTO thyristor can be conceptualized as comprising an npn transistor and a pnp transistor, interconnected as shown in Figure 1.

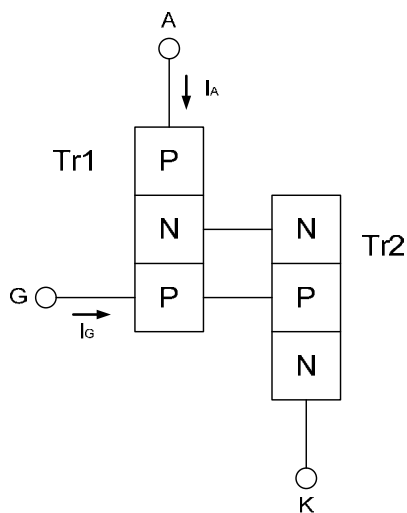


Fig. 1. Two transistor model

Here, the collector of the npn transistor provides base-drive to the pnp, while the collector of the pnp, along with any externally supplied gate current, furnishes base current to the npn. In this positive feedback arrangement, regeneration occurs once the loop gain exceeds one, when each transistor drives its "mate" into saturation.

The GTO thyristor model is then connected to the gate circuit with its operation circuit parameters, shown in Figure 2 and Table 1.

Operation Circuit	Ld	1 μ H
	Rd	20 Ω , 10 Ω , 5 Ω
	Vd	100V
GTO	PNP	SMBT3906
	NPN	SMBTA06
	R	1 Ω
Gate Circuit	Von	10V
	Voff	-60V
	Ron	40 Ω
	Roff	22 Ω , 10 Ω , 5 Ω

Table 1. Operation circuit parameters of GTO thyristor

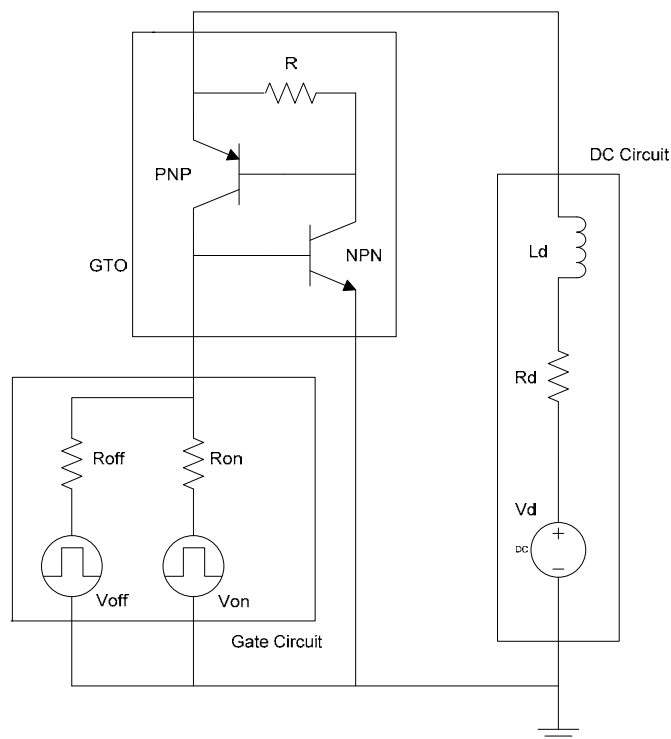


Fig. 2. GTO thyristor model and its operation circuit

In this simulation, we are using the Texas Instrument of SMBTA06 and SMTB3906 for the NPN and PNP transistors. Turn-on and turn-off of GTO thyristor model are controlled by connecting the gate terminal to the gate circuit. GTO thyristor will turned on when positive gate pulse current is applied. Small gate pulse current is enough to turn it on. Here, we set the gate pulse current 5% of the anode current. Meanwhile, GTO thyristor will turned off when negative gate pulse current is applied. Here, we set the gate pulse current 60% of the anode current. Normally, the gate current required to turn it off may be as much as 20% of the anode current. In this paper, we want to consider the turn-off time, where at 60% of anode current, the turn-off time is smaller than at 20% of anode current.

Simulation has been done with PSPICE simulator, and Figure 3, Figure 4 and Figure 5 show the waveform characteristics of the GTO thyristor with anode current 5A, 10A and 20A, respectively. Here, we applied 100V of anode-cathode voltage to the GTO thyristor model. From the figures, we measured the storage time, fall time, tail time and turn-off time. All the measured values are stated in Table 2. We set the turn-on time delay at 2.0 μ s and turn-off time delay at 10 μ s. These time delay settings are very important in the switching operation of 6 pulse GTO thyristor converter circuit. From these results, we know that GTO thyristor can be turned on and turned off in the range current of 5A ~ 20A with a small turn-off time. This GTO thyristor model will be used and implemented in the 6 pulse converter circuit.

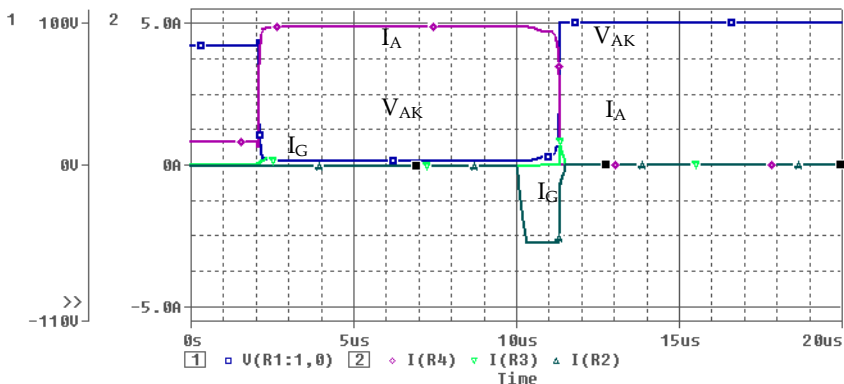


Fig. 3. Turn-on and turn-off characteristics of GTO thyristor ($I_d=5A$)

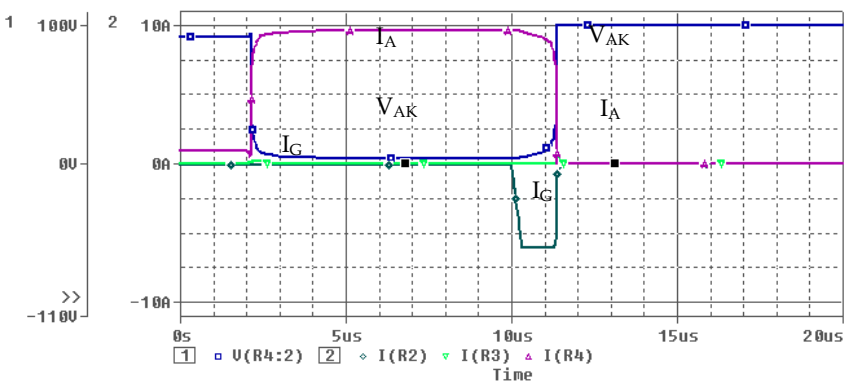


Fig. 4. Turn-on and turn-off characteristics of GTO thyristor ($I_d=10A$)

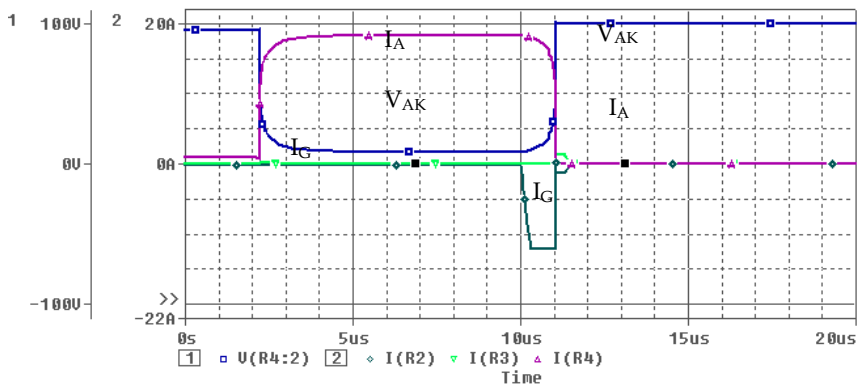


Fig. 5. Turn-on and turn-off characteristics of GTO thyristor ($I_d=20A$)

Anode Current [A]	Storage Time [μ s]	Fall Time [μ s]	Tail Time [μ s]	Turn-off Time [μ s]
5	1.191	0.140	0.002	1.333
10	0.977	0.396	0.002	1.375
20	0.573	0.830	0.002	1.405

Table 2. Storage time, fall time, tail time and turn-off time for a different anode current

3.6 pulse converter circuit

Consider the Figure 6 in which a 3 phase, 6 pulse converter supplies power to a load. Each three single phase power supply, V_x , V_y and V_z fed 50V and 50Hz of ac voltage and frequency. The other parameters in the ac side are shown in Table 3. 6 pulse converter circuit consist of 6 GTO thyristors, and each GTO thyristors are triggered by the gate circuit G1 ~ G6. The gate circuit parameters for this simulation are the same as in Table 1, explained above. At the dc side, the load is composed of a dc voltage V_d and a variable resistor R_d in series with a smoothing inductor L_d . The parameters of these components are also shown in Table 3. The value of variable resistor is varying to fix a value of dc output current at one level. 6 pulse converter can be functioned as a rectifier and an inverter depend on the firing angle, α . It is function as a rectifier when the firing angle is in the range of $0^\circ \sim 90^\circ$. When the firing angle is advance from 90° , the converter will function as an inverter. Therefore, dc voltage, V_d is required during the inverter operation. So, the dc voltage value is varying in the range of $1\mu V \sim 200V$ for this simulation.

3 Phase Circuit (AC Side)	Rx, Ry, Rz	0.1m Ω
	Lx, Ly, Lz	0.1mH
	Vx, Vy, Vz	50V, 50Hz
6 Pulse Converter	G1 ~ G6	Gate Circuit
DC Side	Rd	Variable
	Ld	1mH
	Vd	1 μ V ~ 200V

Table 3. Parameters of 6 pulse converter circuit

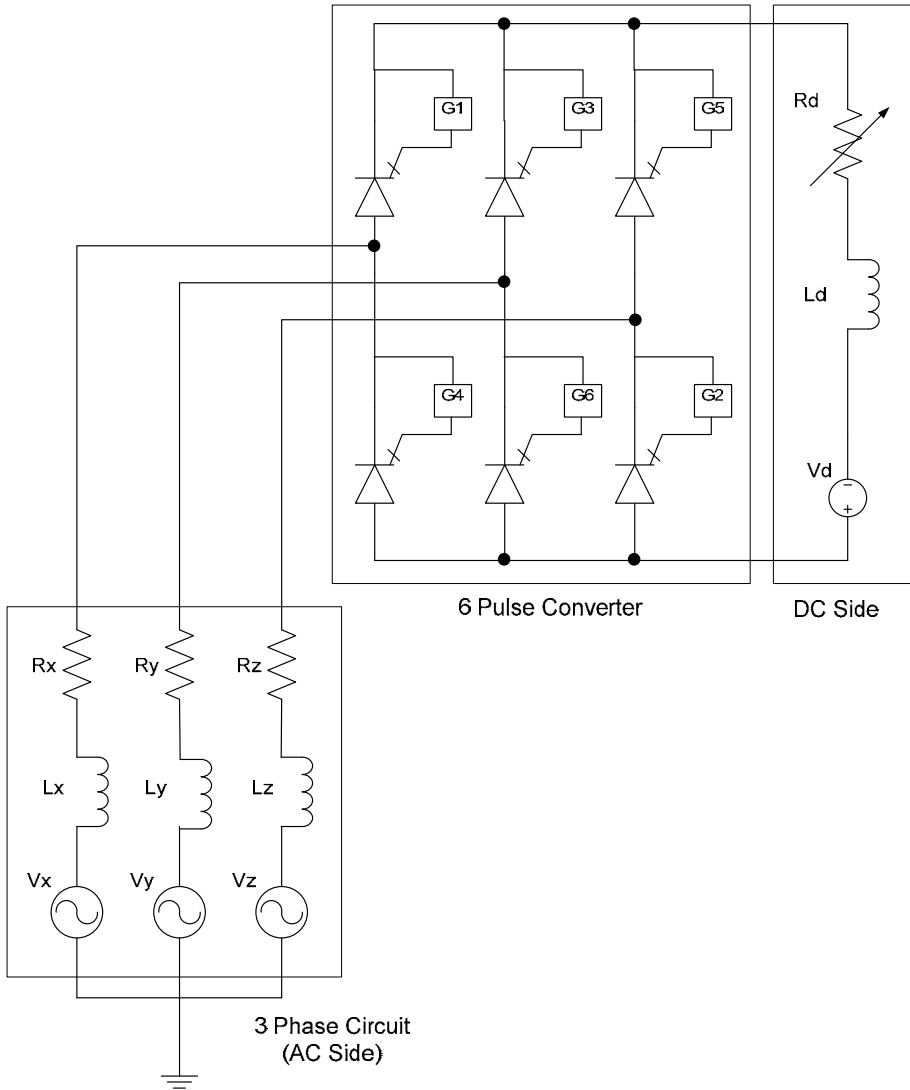
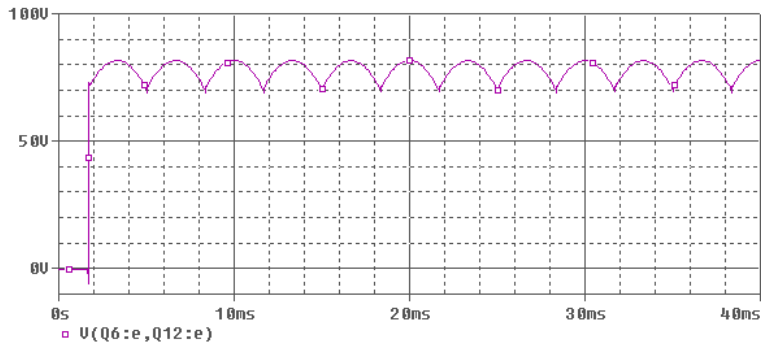


Fig. 6. 6 pulse converter circuit

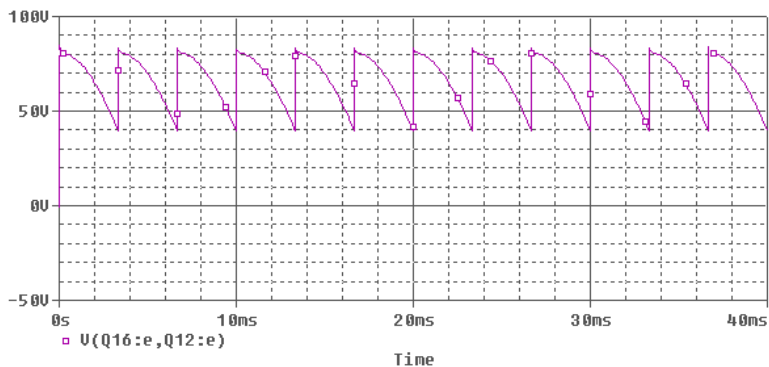
Figure 7 shows some examples of dc output voltages at different firing angles and the dc output current is fixed to 5A. The time delays are setting depend on the required firing angle. For example, if we want to turn-on GTO thyristor with gate circuit G1 at firing angle $\alpha = 15^\circ$, we need to fired a positive gate current at time delay, $TD=2.5ms$. The simple equation is given as (T. Wildi, 2006),

$$TD = \frac{\alpha + 30^\circ}{360^\circ} \times \frac{1}{f} \tag{1}$$

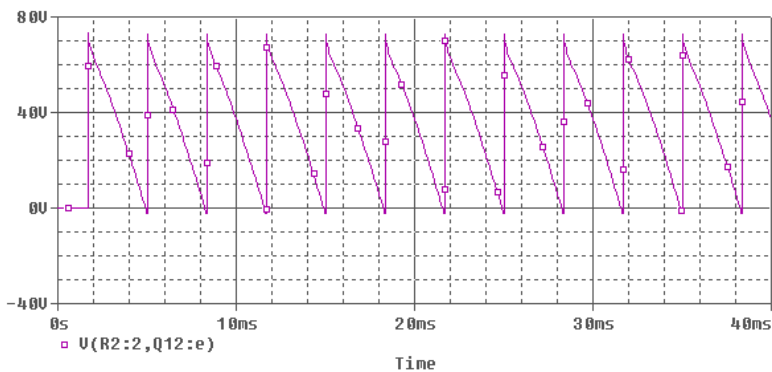
where, f : supply frequency



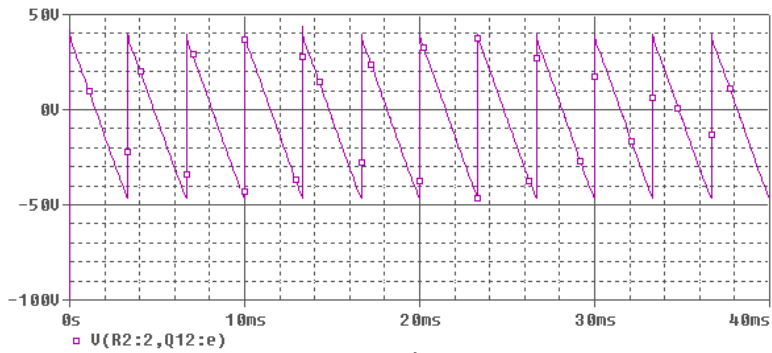
(a) $\alpha = 0^\circ$



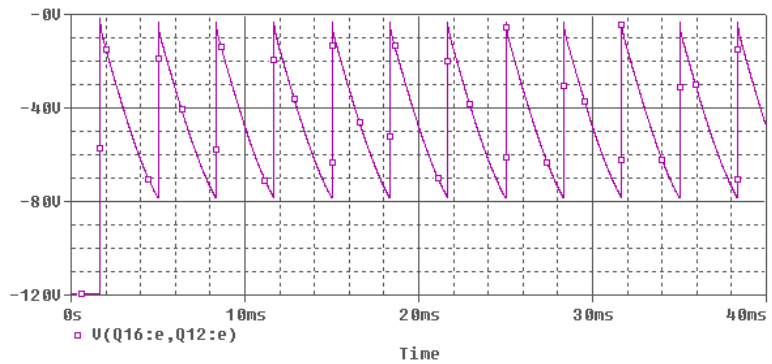
(b) $\alpha = 30^\circ$



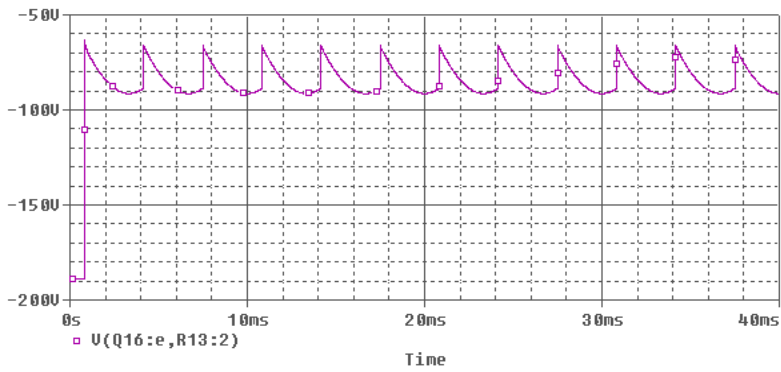
(c) $\alpha = 60^\circ$



(d) $\alpha = 90^\circ$



(e) $\alpha = 120^\circ$



(f) $\alpha = 165^\circ$

Fig. 7. DC output voltages at different α ($I_d=5A$)

We make an analysis of the relation between firing angle and dc output voltage. Using the 6 pulse converter circuit in Figure 18, and varying the firing angle α in the range of $0^\circ \sim 165^\circ$ (this range is taken after considered the commutation overlap), we measured the simulation results of dc output voltage. These simulation results are compared with mathematical calculation results. For mathematical calculation, the dc output current is given as,

$$I_d = \sqrt{\frac{3}{2}} I_m \left\{ \cos\left(\alpha + \frac{\pi}{2} - \phi\right) - \cos\left(\alpha + \mu + \frac{\pi}{2} - \phi\right) \right\} \quad (2)$$

rearrange it,

$$\cos\left(\alpha + \frac{\pi}{2} - \phi\right) - \cos\left(\alpha + \mu + \frac{\pi}{2} - \phi\right) = \frac{2I_d}{\sqrt{3}I_m} \quad (3)$$

and dc voltage is given as,

$$E_{dc} = \frac{3\sqrt{3}}{2\pi} E_m (\cos\alpha + \cos(\alpha + \mu)) \quad (4)$$

where, I_m : maximum ac current, E_m : maximum ac voltage, α : phase control angle, μ : overlap angle

From equation (10), if we change to the form of $\cos(\alpha + \mu)$, it will become as,

$$\cos(\alpha + \mu) = \cos\left\{ \phi - \frac{\pi}{2} + \cos^{-1}\left(\cos\left(\alpha + \frac{\pi}{2} - \phi\right) - \frac{2I_d}{\sqrt{3}I_m} \right) \right\} \quad (5)$$

adding $I_m = \frac{E_m}{\sqrt{R^2 + (\omega L)^2}}$ into equation (13) and times (\cos^{-1}) both right and left, we will get,

$$\alpha + \mu = \phi - \frac{\pi}{2} + \cos^{-1}\left(\cos\left(\alpha + \frac{\pi}{2} - \phi\right) - \frac{2I_d \sqrt{R^2 + (\omega L)^2}}{\sqrt{3}E_m} \right) \quad (6)$$

where, I_d : dc current, $\phi = \tan^{-1} \frac{\omega L}{R}$

Insert all parameters given in Table 6 into equation (14) will become as follow,

$$\alpha + \mu = -0.1520^0 + \cos^{-1}\left(\cos\left(\alpha + 0.1520^0\right) - 0.0009I_d \right) \quad (7)$$

The result of mathematical calculation is determined by the equation (1), equation (4) and equation (7). Figure 8, Figure 9 and Figure 10 show the dc output voltage vs. firing angle at dc output current of 1A, 5A and 10A respectively. From these figures, we know that the curves of simulation results and mathematical calculation results are almost same. The

values of dc output voltages are not too much different in each firing angle except in the range of $0^\circ \sim 75^\circ$, where the values of the simulation results are little bit smaller than the mathematical calculation results. It is may be happened due to some reason such as voltage drop during the turn-on and turn-off operation of the GTO thyristors, power losses due to commutation overlap and measurement error in maintaining the same level of dc output current during the simulation. From Figure 8, Figure 9 and Figure 10, we know that power transfer can be controlled by varying the firing angle, and power transmission direction can be feed either to the dc side or to the ac side. So, the 6 pulse converter circuit can be functioned either as a rectifier or an inverter.

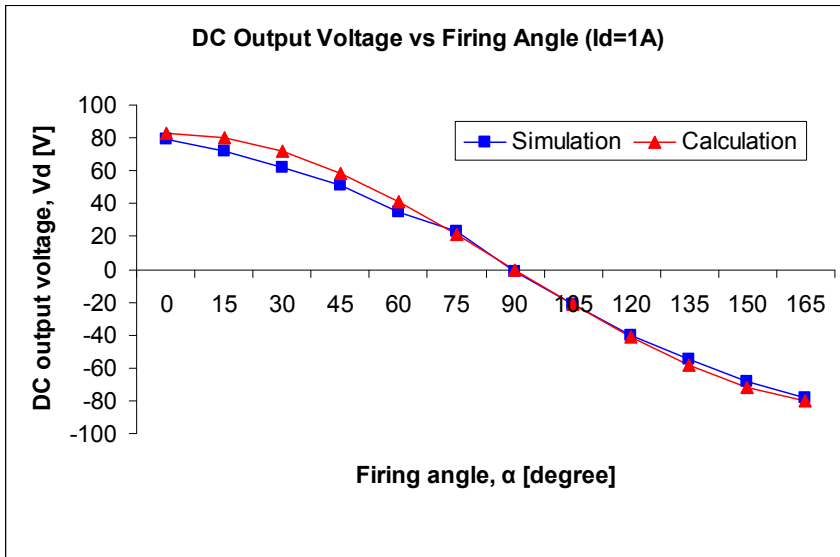


Fig. 8. DC output voltage vs. firing angle ($I_d=1A$)

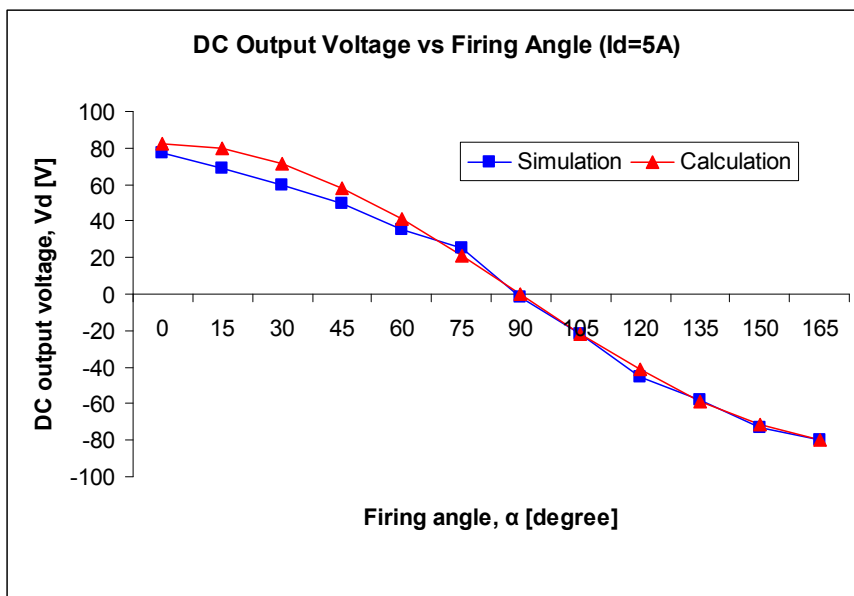


Fig. 9. DC output voltage vs. firing angle (Id=5A)

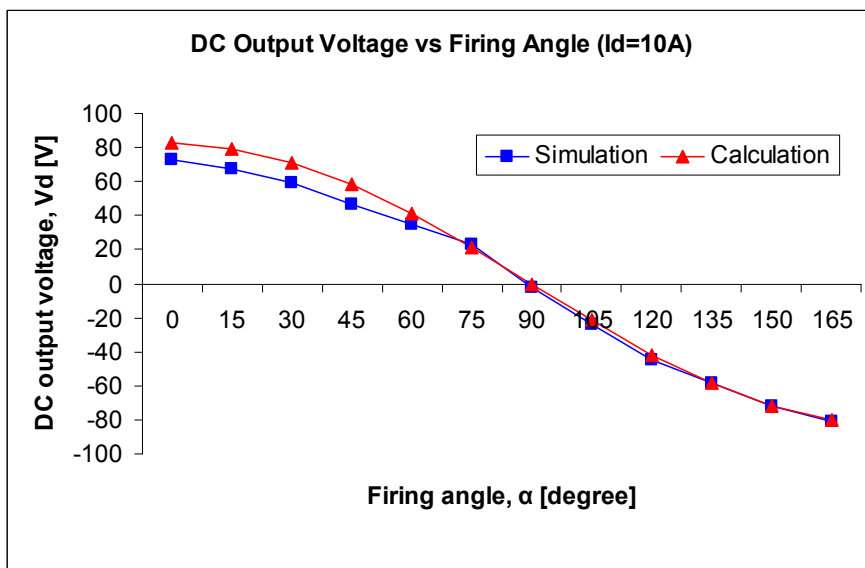


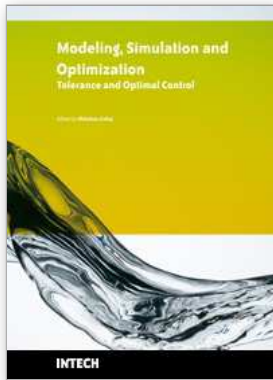
Fig. 10. DC output voltage vs. firing angle (Id=10A)

4. Conclusion

Using PSPICE simulator we create GTO thyristor model with its gate circuit and obtained the switching characteristics. We know that GTO thyristor can be turned on and turned off in the range current of 5A ~ 20A with a small turn-off time. This GTO thyristor model is being implemented in the 6 pulse converter circuit with controlled gate circuits. The characteristics curves of firing angle vs. dc output voltage show almost the similar characteristics except in the range of firing angle $0^{\circ} \sim 75^{\circ}$, where the simulation results are little bit smaller compared to the mathematical calculation results. We also know that power transfer can be controlled either as a rectifier or an inverter.

5. References

- T. Wildi (2006). *Electrical Machine, Drives and power systems*, Prentice Hall, 0131969188 , USA.
- Kaz Furmanczyk & Mark Stefanich (2004). Demonstration of Very High Airbone AC to DC Converter, *Crane Aerospace and Electronics Conference*, pp. 3210-3215, 2004-01-3210, November 2004, USA.
- F. Schettler; H. Huang & N. Christl (2000). HVDC Transmission System using Voltage Sourced Converters - Design and Applications, *Power Engineering Society Summer Meeting*, pp. 715-720, 078036420, 16-20 July 2000, IEEE
- Thadiappan Krishnan & Bellamkonda Ramaswami (1974). A Fast Response DC Motor Speed Control System, *IEEE Transaction on Industry Applications*, pp. 643-651, 349214, September/October 1974, IEEE.
- Z. Zabar & A. Alexandrovitz (1970). Guidelines on Adaption of Thyristorized Switch for DC Motor Speed Control, *IEEE Transaction on Industrial Instrumentation*, pp. 10-13, 229594, February 1970, IEEE.



Modeling Simulation and Optimization - Tolerance and Optimal Control

Edited by Shkelzen Cakaj

ISBN 978-953-307-056-8

Hard cover, 304 pages

Publisher InTech

Published online 01, April, 2010

Published in print edition April, 2010

Parametric representation of shapes, mechanical components modeling with 3D visualization techniques using object oriented programming, the well known golden ratio application on vertical and horizontal displacement investigations of the ground surface, spatial modeling and simulating of dynamic continuous fluid flow process, simulation model for waste-water treatment, an interaction of tilt and illumination conditions at flight simulation and errors in taxiing performance, plant layout optimal plot plan, atmospheric modeling for weather prediction, a stochastic search method that explores the solutions for hill climbing process, cellular automata simulations, thyristor switching characteristics simulation, and simulation framework toward bandwidth quantization and measurement, are all topics with appropriate results from different research backgrounds focused on tolerance analysis and optimal control provided in this book.

How to reference

In order to correctly reference this scholarly work, feel free to copy and paste the following:

Muhamad Zahim Sujod (2010). Modelling and Simulation of 6 Pulse GTO Thyristor Converter, Modeling Simulation and Optimization - Tolerance and Optimal Control, Shkelzen Cakaj (Ed.), ISBN: 978-953-307-056-8, InTech, Available from: <http://www.intechopen.com/books/modeling-simulation-and-optimization-tolerance-and-optimal-control/modelling-and-simulation-of-6-pulse-gto-thyristor-converter>

INTECH
open science | open minds

InTech Europe

University Campus STeP Ri
Slavka Krautzeka 83/A
51000 Rijeka, Croatia
Phone: +385 (51) 770 447
Fax: +385 (51) 686 166
www.intechopen.com

InTech China

Unit 405, Office Block, Hotel Equatorial Shanghai
No.65, Yan An Road (West), Shanghai, 200040, China
中国上海市延安西路65号上海国际贵都大饭店办公楼405单元
Phone: +86-21-62489820
Fax: +86-21-62489821

© 2010 The Author(s). Licensee IntechOpen. This chapter is distributed under the terms of the [Creative Commons Attribution-NonCommercial-ShareAlike-3.0 License](#), which permits use, distribution and reproduction for non-commercial purposes, provided the original is properly cited and derivative works building on this content are distributed under the same license.